

Aramid Nanofiber Composite Conductive Film Prepared via a Simple Method^①

HUANG Jia-Jing^{a, b} WANG Ting^{b, c}
SU Yu-Miao^{b, c} TU Chao-Yang^{b②} LI Wen-Mu^{b, d②}

^a (College of Chemistry and Materials Science, Fujian Normal University, Fuzhou 350007, China)

^b (Key Laboratory of Optoelectronic Materials Chemistry and Physics, Fujian Institute of Research on the Structure of Matter, Chinese Academy of Sciences, Fuzhou 350002, China)

^c (University of Chinese Academy of Sciences, Beijing 100049, China)

^d (Innovation Academy for Green Manufacture, Chinese Academy of Sciences, Beijing 100190, China)

ABSTRACT It is very hard to obtain uniformly dispersed conductive polymer nanocomposites because of the accumulation tendency of nanomaterials. In current work, the aramid nanofiber/silver nanowire composite film was prepared by mixing evenly through the solution and then vacuum filtration. The composite film exhibited desirable physical properties such as high tensile strength (121 MPa), outstanding electrical conductivity (652 S cm^{-1}), and thermal conductivity ($0.12 \text{ W m}^{-1} \text{ K}^{-1}$). These endow our aramid nanofiber/silver nanowire composite film with possible applications in infrared stealth and harsh environments.

Keywords: polymer nanocomposites, aramid nanofiber, silver nanowire;

DOI: 10.14102/j.cnki.0254-5861.2011-3154

1 INTRODUCTION

In recent years, people's enthusiasm for flexible electronic products is increasing with the development of smartphones^[1]. Indium tin oxide (ITO) is used as a conductive material^[2]. However, ITO still has some shortcomings, such as high preparation cost, harsh preparation conditions, complex process, increasing shortage of raw material indium (In), and poor flexibility at present. Therefore, the researches on finding alternative materials for ITO have never stopped^[3]. Conductive polymer composite nanomaterial is a potential alternative material. Polymer-based conductive composites are high-performance multi-functional composites formed by introducing fillers into the polymer matrix^[4]. It is one of the most concerned research fields in nanotechnology and composites. Conductive polymer composites have become a hot research direction because they are designable, easy to process, and widely used (such as sensors, electrodes, electromagnetic shielding, etc.)^[5].

Nano-conductive fillers (graphene, carbon nanotubes, MXene, and their mixtures) have been studied and applied in polymer composites^[6]. Li et al. prepare high-density thin-layer Graphite foam-based composite architectures with superior compressibility and excellent electromagnetic interference shielding performance (up to 36.1 dB)^[7]. Zeng et al. develop lightweight and anisotropic porous MWCNT/WPU composites with electrical conductivity (44 S m^{-1}) via freeze-drying^[8]. Liao et al. make conductive MXene nanocomposite organohydrogel for flexible, healable and low-temperature tolerant strain sensors^[9].

Silver nanowire (AgNW) is a kind of one-dimensional nanomaterials with good light transmittance, electrical conductivity, and stability^[10]. Silver nanowires have not only excellent electrical conductivity of silver but also excellent light transmittance and flexural resistance because of the size effect at the nanometer level^[11].

Therefore, it is regarded as the most likely material to replace the traditional ITO transparent electrode, which pro-

Received 23 February 2021; accepted 18 March 2021

① The authors gratefully acknowledge the Innovation Academy for Green Manufacture, Chinese Academy of Sciences (IAGM2020C22), the Fujian STS plan supporting project (Nos. 2019T3005, 2019T3014, 2019T3034), the 100-Talent Program of the Chinese Academy of Sciences, and the High-level Talents for Entrepreneurship and Innovation of Fujian Province

② Corresponding authors. Li Wen-Mu, Professor. E-mail: liwm@fjirsm.ac.cn; Tu Chao-Yang, Professor. E-mail: tcy@fjirsm.ac.cn

vides the possibility of realizing flexible LED display, touch screen, and so on, and a large number of studies have applied it to thin film-solar cells. In addition, owing to the large aspect ratio effect, silver nanowires also have outstanding advantages in the application of conductive adhesive and thermally conductive adhesive^[12]. AgNW-based polymer composites have also made new progress. Zhu *et al.* report a kind of printable elastic silver nanowire-based conductor for washable electronic textiles^[13].

Aramid fiber is a high-tech synthetic fiber made from aromatic compounds by polycondensation spinning, which is called aromatic polyamide fiber. Aramid has excellent properties such as lightweight, flame retardant, temperature resistance, insulation, radiation resistance, high strength, high elastic modulus, etc., and is widely used in military defense, security protection, aerospace, environmental protection, electronic and electrical materials, and other fields^[14]. Aramid nanofibers (ANF) have dual characteristics of both aramid and polymer nanofibers, so they can be used as polymer matrix to solve the problem of the poor composite effect of aramid itself^[15]. Ma *et al.* report an ultraflexible, heat-resistant, and mechanically strong ANF/AgNW nanocomposite paper with AgNW embedded structure^[16]. However, this method is not suitable for recycling materials.

Therefore, we report a recyclable aramid nanofiber/silver nanowire composite conductive film by vacuum-assisted filtration. Through the study, AgNW forms a connection with aramid nanofibers through hydrogen bonding, which is well dispersed in the polymer matrix, showing good mechanical properties (tensile strength of 121 MPa), electrical conductivity (652 S cm^{-1}), and thermal insulation ($0.12 \text{ W m}^{-1} \text{ K}^{-1}$). This provides the possibility for the application of the film. At the same time, the possibility of recycling of the film is also made by the emerging alkali dissolution method.

2 EXPERIMENTAL

2.1 Materials preparation

Short-cut aramid fiber purchased from DuPont, USA. Silver nitrate (AgNO_3), ethylene glycol (EG), copper chloride dihydrate ($\text{CuCl}_2 \cdot 2\text{H}_2\text{O}$), potassium hydroxide (KOH), dimethyl sulfoxide (DMSO), and PVP ($M_w \approx 300,000$) of analytical grade for the preparation of silver nanowires were used as received without further purification.

2.2 Fabrication of the ANF suspension

The dispersion of aramid nanofiber (2 mg mL^{-1}) was synthesized according to the previous reports^[15]. Typically, 2 g aramid short cut fiber and 3 g KOH, 1000 mL DMSO are mixed. Next, 40 mL deionized water was added and sealed. Stir until the fiber completely dissolves to form a transparent solution.

2.3 Fabrication of the AgNW suspension

AgNWs were synthesized by modified polyol process using one-pot process^[17]. In this work, 100 mL of ethylene glycol (EG), 0.8 g of polyvinylpyrrolidone ($M_w \approx 300,000$) and 1 g of silver nitrate (AgNO_3) were sequentially dissolved using a magnetic stirrer. The stirrer was carefully removed from the mixture solution once all chemicals were thoroughly dissolved. Then, 1.6 mL of as-prepared $\text{CuCl}_2 \cdot 2\text{H}_2\text{O}$ (3.3 mM) solution in EG was rapidly injected into the mixture and stirred mildly. Lastly, the mixture solution was immersed in a preheated silicone oil bath at 130°C . The growth of AgNWs in the mixture was proceeded at the elevated temperature for 1.5 h. Finally, the mixture was washed with acetone and ethanol, filtered by vacuum, and dried in vacuum at 60°C for 24 h. The resulting solids were re-dispersed in DMSO to obtain the AgNW dispersion (4 mg mL^{-1}).

2.4 Fabrication of the ANF/AgNW film

First, ANF and AgNW dispersions were mixed in different proportions. Then, under stirring, the dispersion is injected into the deionized water through a syringe to form a colloidal dispersion. Finally, the colloidal dispersion was filtered in vacuum and dried by infrared lamp. The ANF/AgNW film can fall off naturally from the top of the filter membrane. According to the mass fraction of AgNW, the sample is defined as ANF, AA-18, AA-30, and AA-40, respectively.

2.5 Characterization

The morphologies and microstructures of ANF film are obtained by Scanning electron microscopy (SEM) measurements conducted with a field-emission scanning electron microscope (SU8010, Hitachi), and those of AgNW and AA film are obtained by Sigma 300 SEM. Atomic force microscope (AFM) photograph of ANF was characterized using a Scanning Probe Microscope (SPM) Dimension ICON. X-ray diffraction (XRD) patterns of AgNW, ANF film, AA film and so forth were recorded in the 2θ range ($5^\circ \sim 65^\circ$) using a MiniFlex-II diffractometer (Rigaku, Japan). AgNW, ANF film, AA film, etc. were characterized with a VERTEX 70 Fourier-transform infrared (FT-IR) spectrometer. Electrical conductivities of the AA films were conducted with a Four Probes Tech RST-8 resistivity meter (China,

Guangzhou). The tensile strength of the film is measured by SUNDOSPI tester. Thermal conductivity was measured with TC3000E. The infrared thermal imaging map was taken by infrared thermal imaging camera HT-18.

3 RESULTS AND DISCUSSION

3.1 Synthesis of the ANF suspension

The dispersion of aramid nanofibers is to obtain by alkaline solution (KOH solution of DMSO) in this work (Fig. 1a). This method has the advantages of simplicity, low energy

consumption, and safety, and can provide a basis for the sustainable use of aramid. The specific process is to convert large-scale aramid fiber into nanometer aramid fiber by weakening the hydrogen bond and enhancing the electrostatic repulsion between polymer chains. The obtained dispersion is transparent and accompanied by the Tyndall effect (Fig. 1a)^[18]. As the concentration increases, the color increases to crimson. A colloidal dispersion is formed by injection in deionized water, which is also accompanied by the Tyndall effect (Fig. 1b). The morphology of ANF can be observed by AFM (Fig. 1c).

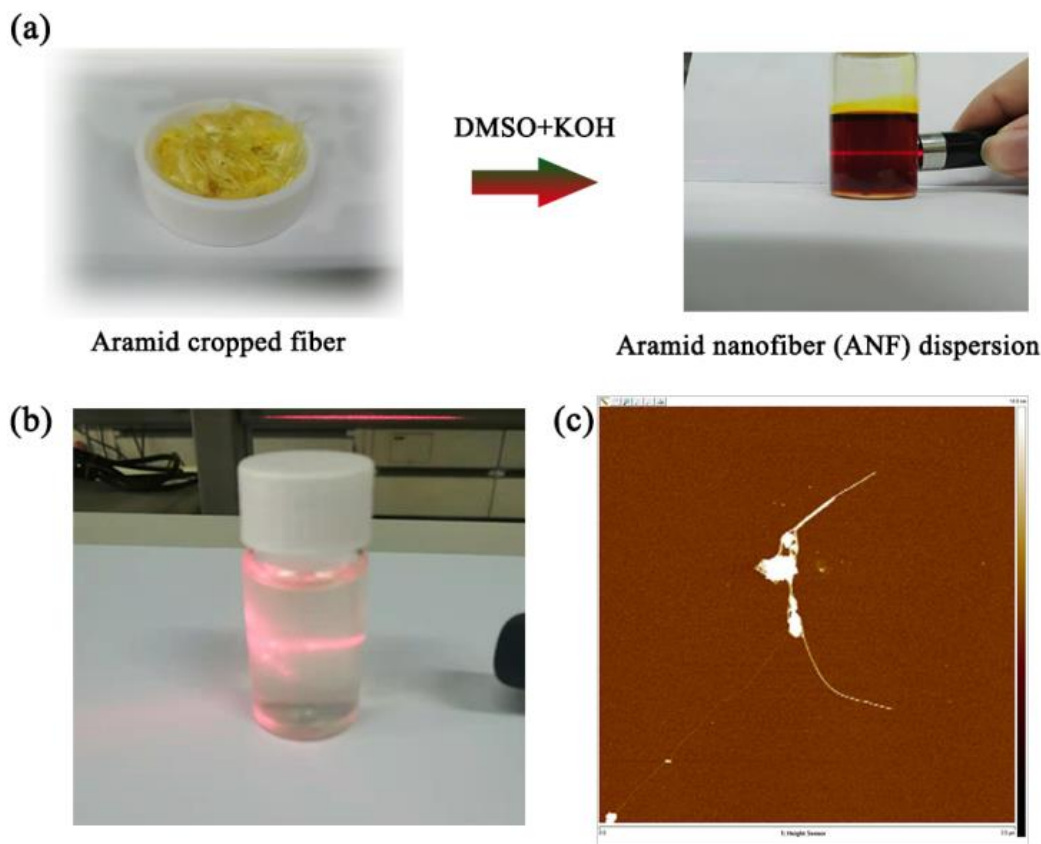


Fig. 1. (a) Process of preparing aramid nanofiber (ANF) dispersion; (b) Tyndall effect of ANF water dispersion; (c) AFM images of ANF

3.2 Synthesis of the AgNW suspension

AgNWs were synthesized by the improved polyol one-pot method. The obtained AgNW dispersion is grayish-white (Fig. 2a)^[19]. At lower concentrations, AgNW dispersion can also have the Tyndall effect (Fig. 2b)^[20]. The qualitative characterization of AgNW can be proved by XRD (Fig. 2c). From the XRD image, we can see that the characteristic peaks of AgNW (111), (200), (220), (311), and (222) exist

with no extra peaks, indicating the successful acquisition of AgNW^[21]. From the SEM image, we can see that AgNW is distributed linearly (Fig. 2d). Among them, the length and size of AgNW are not consistent. However, from the measured area, you can see that the length of AgNW is 3.554 to 6.200 μm in size. The diameters of AgNW are all less than 100 nm. To sum up, the AgNW is successfully achieved, but the aspect ratio is not uniform.

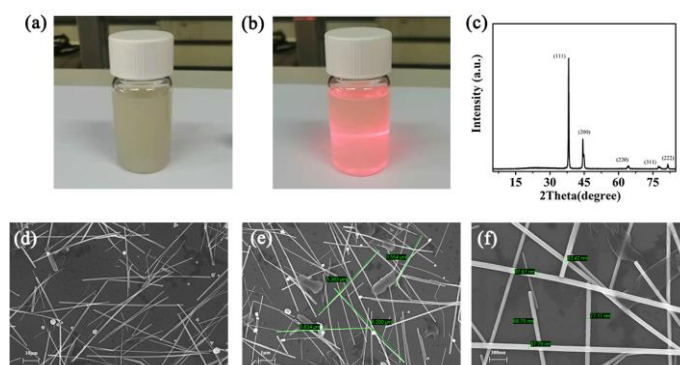


Fig. 2. (a) Photograph of AgNW dispersion; (b) Tyndall effect of AgNW dispersion; (c) XRD pattern of AgNW; (b-f) SEM images of AgNW

3.3 Preparation and properties of AA films

3.3.1 Synthesis of the AA film

The process of preparing AA film is shown in Fig. 3. First, AgNW and ANF dispersion is mixed uniformly. Then, under stirring, the dispersion is injected into deionized water through a syringe to form a colloidal dispersion. Then, the

mixed solvent is removed by vacuum extraction and filtration device. The colloidal solution can be filtered to remove excess DMSO to form bulk colloids for easy transport. Finally, the AA film can fall off naturally under the drying of infrared lamps or natural drying for 24 hours.

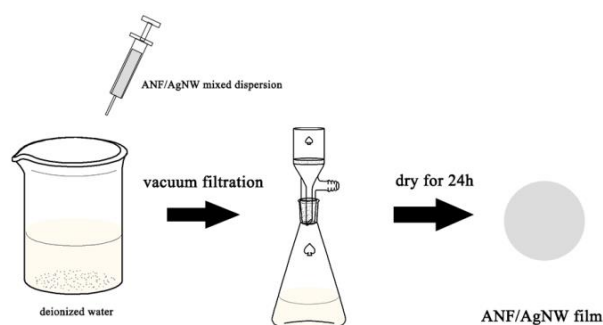


Fig. 3. Schematic method for the fabrication of ANF/AgNW film

3.3.2 Characterization of the ANF and AA films

From Fig. 4, a yellow translucent film with 30 μm thickness can be obtained from pure ANF dispersion. The reason for showing yellow is the characteristic color of the aramid itself. The translucent property makes the aramid

nanofiber film have application prospects. From the SEM image of the surface of the ANF film, it can be seen that the surface as a whole is flat and there are no obvious defects. In contrast, the AA film shows that AgNW is successfully dispersed in the aramid film and forms a conductive path.

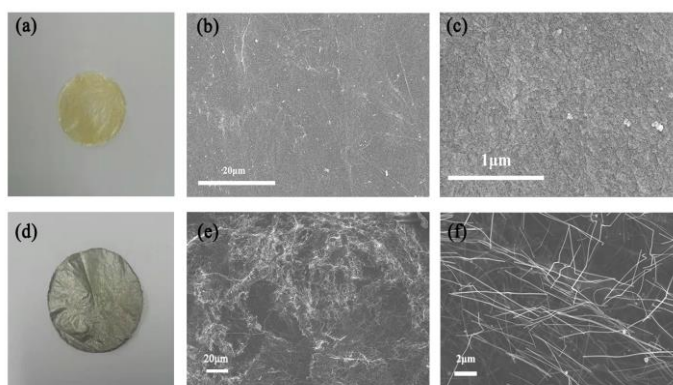


Fig. 4. (a) Photograph of ANF film; (b) and (c) SEM images of the surface of ANF film; (d) Photograph of AA film; (e) and (f) SEM images of the surface of AA film

Fig. 5a shows the XRD patterns of ANF, AgNW, and AA films. There is no obvious characteristic peak in ANF film. The diffraction peak and crystal plane of AA film are similar to those of AgNW, and its intensity is weaker than that of AgNW, which proves that AgNW exists completely in a polymer matrix^[16]. As shown in Fig. 5b, 1629 cm^{-1} of the characteristic peak in the FT-IR spectrum of AgNW

originates from the carbonyl group of PVP on its surface. For ANF films, the characteristic peaks of 1643, 1540, and 3329 cm^{-1} correspond to the carbonyl and N-H groups, respectively^[16]. The characteristic peak of the N-H group (3320 cm^{-1}) of AA film is smaller than that of ANF film, which proves that a hydrogen bond is formed between ANF and AgNW. This is simply shown in Fig. 6.

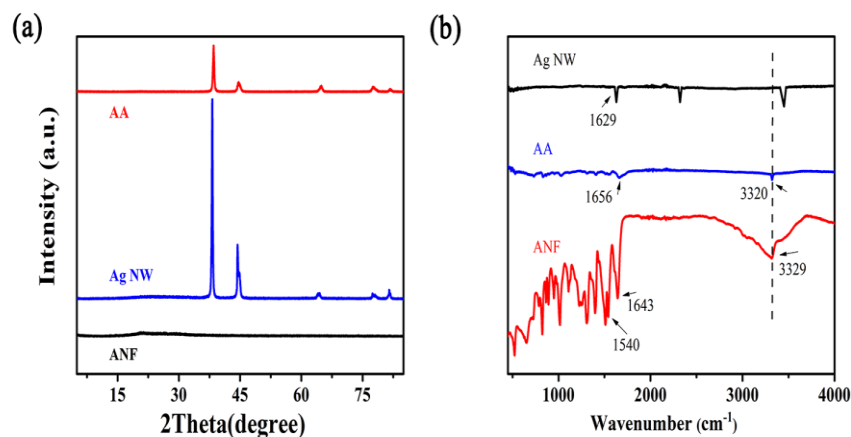


Fig. 5. (a) XRD pattern of ANF, AgNW and AA films; (b) FT-IR spectroscopy of ANF, AgNW and AA films

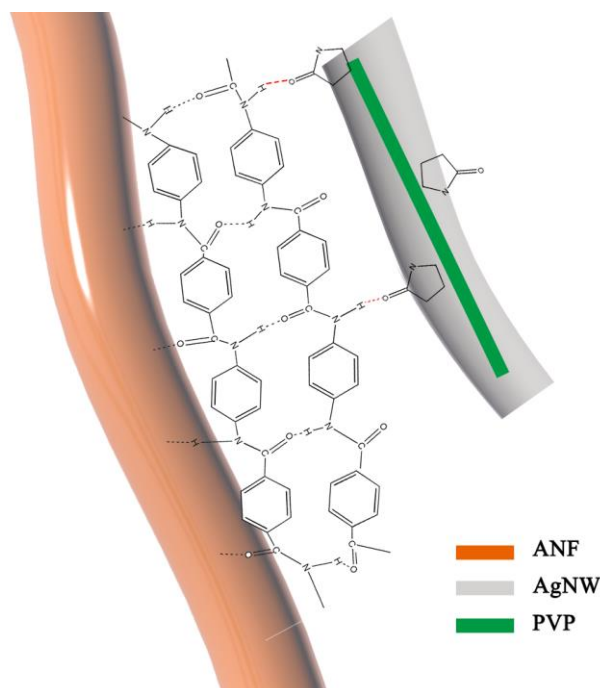


Fig. 6. Hydrogen bonds between ANF and PVP

3.3.3 Performance of the ANF and AA films

Fig. 7a shows the curves of tensile force and strain of ANF and AA-40 films. It can be seen from the figure that the tensile strength of ANF film can reach 124 MPa, while that of AA-40 film decreases to 121 MPa. The decrease of the

tensile strength of the composite film may be the reason that the increase of mass fraction of AgNW leads to the aggregation of AgNW more easily. The decrease of composite film is not very obvious. This mechanical property makes the composite film more durable, especially in harsh

environments^[22, 23]. The composite film has not only excellent mechanical properties but also flexibility (Fig. 7b).

Aramid is an excellent electrical insulating material^[24], so its conductivity can not be measured on the conductivity tester (Fig. 7c). With the increase of mass fraction of AgNW, the conductivity of AA composite film has increased from 35 to 652 S cm⁻¹. Among them, the increase of electrical conductivity is the most obvious from AA-18 to AA-30,

indicating that AgNW forms a more complete conductive network in the ANF matrix, and the barrier effect of ANF decreases. The film is connected to the LED in a simple circuit. The brightness of LED can represent the conductivity of the film. The high conductivity of AA composite film lays a foundation on its probable applications such as electromagnetic shielding materials, sensors, energy storage, and so on.

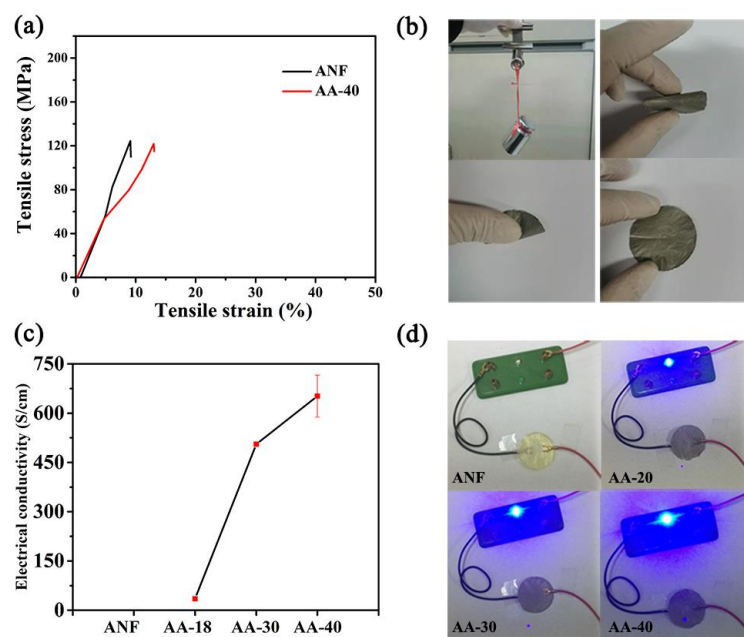


Fig. 7. (a) Tensile stress-strain curves of ANF and AA films; (b) Excellent flexibility and high strength of AA film; (c) Electrical conductivities of ANF and AA films; (d) Different brightness of LED light connected with ANF or AA film

Aramid is also an excellent thermal insulation material^[25]. Fig. 8a shows that the thermal conductivity of ANF film is 0.1120 W m⁻¹ K⁻¹ when its thickness is only 30 μm. As a metal filler, AgNW has excellent heat transfer performance. Therefore, with the increase of filling amount, thermal conductivity of the composite membrane increased from 0.1133 to 0.1213 W m⁻¹ K⁻¹. On the whole, the increase of thermal conductivity is very small and is still within the range

of thermal insulation materials (thermal conductivity less than 0.2). This may be owing to the decrease of heat transfer efficiency due to the excellent thermal insulation performance of ANF as the main matrix is coated with AgNW. From the infrared image, we can know that AA composite film has the possibility of being used as thermal insulation and infrared stealthy materials.

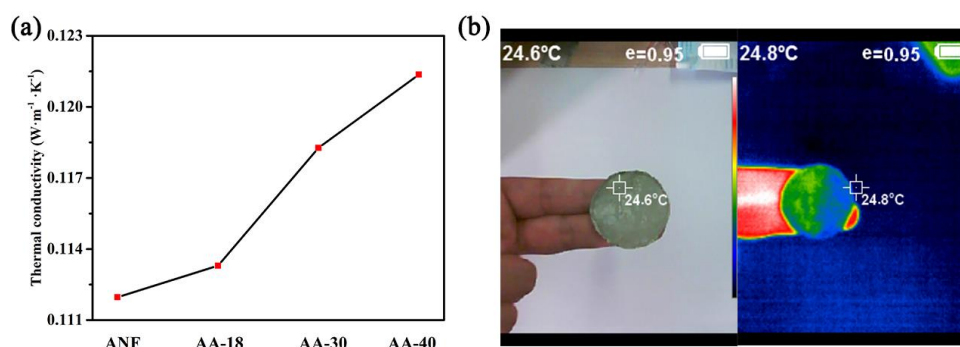


Fig. 8. (a) Thermal conductivities of ANF and AA films, (b) Infrared thermal imaging of AA film

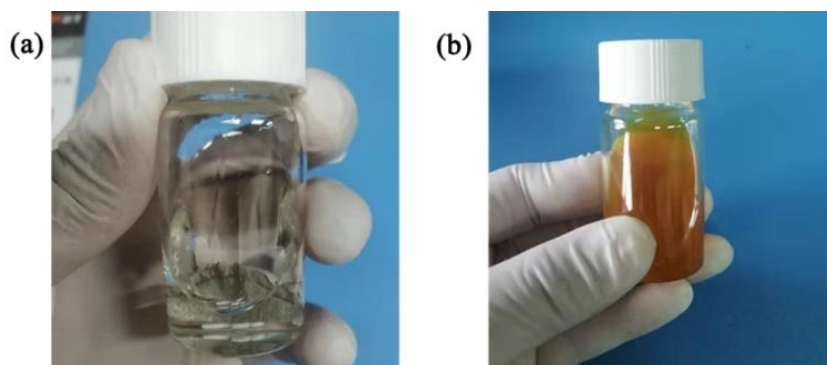


Fig. 9. AA film dissolved in DMSO solution of KOH

The AA film was put into the DMSO solution of KOH and stirred continuously until a turbid orange liquid formed. The orange color of the liquid is derived from the color of the ANF DMSO dispersion. However, the appearance of turbidity is due to the fact that AgNW is also redispersed in it. In the face of the increasingly serious resource crisis, oil shortage has become a major problem that the world must face in the future. Therefore, the solution can be recycled to relieve pressure from the shortage of oil.

4 CONCLUSION

In current work, we provide a recyclable aramid nanofiber/silver nanowire composite conductive membrane by vacuum-assisted filtration. Through the study, AgNW forms a connection with aramid nanofibers through hydrogen bonding, which is well dispersed in the polymer matrix, showing good mechanical properties (tensile strength of 124 MPa), electrical conductivity (652 S cm^{-1}), and thermal insulation ($0.12 \text{ W m}^{-1} \text{ K}^{-1}$). This provides the possibility for the application of membrane. Solution recyclability is conducive to the current trend of sustainable development and the oil crisis.

REFERENCES

- (1) Li, X.; Li, Y.; Guan, T.; Xu, F.; Sun, J. Durable, highly electrically conductive cotton fabrics with healable superamphiphobicity. *ACS Appl. Mater. Interfaces* **2018**, 10, 14, 12042–12050.
- (2) Fu, L. S.; Jiang, J. T.; Zhen, L.; Shao, W. Z. FeNi₃/indium tin oxide (ITO) composite nanoparticles with excellent microwave absorption performance and low infrared emissivity. *Mater. Sci. Eng. B* **2013**, 178, 4, 225–230.
- (3) Wang, Z.; Mao, B.; Wang, Q.; Yu, J.; Dai, J.; Song, R.; Pu, Z.; He, D.; Wu, Z.; Mu, S. Ultrahigh conductive copper/large flake size graphene heterostructure thin-film with remarkable electromagnetic interference shielding effectiveness. *Small* **2018**, 14, 20, 1704332.
- (4) Ru, J.; Fan, Y.; Zhou, W.; Zhou, Z.; Wang, T.; Liu, R.; Yang, J.; Lu, X.; Wang, J.; Ji, C.; Wang, L.; Jiang, W. Electrically conductive and mechanically strong graphene/mullite ceramic composites for high-performance electromagnetic interference shielding. *ACS Appl. Mater. Interfaces* **2018**, 10, 45, 39245–39256.
- (5) Abbasi, H.; Antunes, M.; Velasco, J. I. Recent advances in carbon-based polymer nanocomposites for electromagnetic interference shielding. *Prog. Mater. Sci.* **2019**, 103, 319–373.
- (6) Miao, P.; Wang, J.; Zhang, C.; Sun, M.; Cheng, S.; Liu, H. Graphene nanostructure-based tactile sensors for electronic skin applications. *Nano-Micro Lett.* **2019**, 11, 1.
- (7) Li, H.; Jing, L.; Ngoh, Z. L.; Tay, R. Y.; Lin, J.; Wang, H.; Tsang, S. H.; Teo, E. H. T. Engineering of high-density thin-layer graphite foam-based composite architectures with superior compressibility and excellent electromagnetic interference shielding performance. *ACS Appl. Mater. Interfaces* **2018**, 10, 48, 41707–41716.
- (8) Zeng, Z.; Jin, H.; Chen, M.; Li, W.; Zhou, L.; Zhang, Z. Lightweight and anisotropic porous mwnt/wpu composites for ultrahigh performance electromagnetic interference shielding. *Adv. Funct. Mater.* **2016**, 26, 2, 303–310.
- (9) Liao, H.; Guo, X.; Wan, P.; Yu, G. Conductive mxene nanocomposite organohydrogel for flexible, healable, low-temperature tolerant strain sensors. *Adv. Funct. Mater.* **2019**, 29, 39.
- (10) Zeng, Z.; Wu, T.; Han, D.; Ren, Q.; Siqueira, G.; Nystrom, G. Ultralight, flexible, and biomimetic nanocellulose/silver nanowire aerogels for

- electromagnetic interference shielding. *ACS Nano* **2020**, 14, 3, 2927–2938.
- (11) Zhou, W.; Yao, S.; Wang, H.; Du, Q.; Ma, Y.; Zhu, Y. Gas-permeable, ultrathin, stretchable epidermal electronics with porous electrodes. *ACS Nano* **2020**, 14, 5, 5798–5805.
- (12) Wu, L.; Wang, L.; Guo, Z.; Luo, J.; Xue, H.; Gao, J. Durable and multifunctional superhydrophobic coatings with excellent joule heating and electromagnetic interference shielding performance for flexible sensing electronics. *ACS Appl. Mater. Interfaces* **2019**, 11, 37, 34338–34347.
- (13) Zhu, H. W.; Gao, H. L.; Zhao, H. Y.; Ge, J.; Hu, B. C.; Huang, J.; Yu, S. H. Printable elastic silver nanowire-based conductor for washable electronic textiles. *Nano Res.* **2020**, 13, 10, 2879–2884.
- (14) Yang, B.; Wang, L.; Zhang, M.; Luo, J.; Lu, Z.; Ding, X. Fabrication, applications, and prospects of aramid nanofiber. *Adv. Funct. Mater.* **2020**, 30, 22.
- (15) Yang, B.; Wang, L.; Zhang, M.; Luo, J.; Ding, X. Timesaving, high-efficiency approaches to fabricate aramid nanofibers. *ACS Nano* **2019**, 13, 7, 7886–7897.
- (16) Ma, Z.; Kang, S.; Ma, J.; Shao, L.; Wei, A.; Liang, C.; Gu, J.; Yang, B.; Dong, D.; Wei, L.; Ji, Z. High-performance and rapid-response electrical heaters based on ultraflexible, heat-resistant, and mechanically strong aramid nanofiber/ag nanowire nanocomposite papers. *ACS Nano* **2019**, 13, 7, 7578–7590.
- (17) Jung, J.; Lee, H.; Ha, I.; Cho, H.; Kim, K. K.; Kwon, J.; Won, P.; Hong, S.; Ko, S. H. Highly stretchable and transparent electromagnetic interference shielding film based on silver nanowire percolation network for wearable electronics applications. *ACS Appl. Mater. Interfaces* **2017**, 9, 51, 44609–44616.
- (18) Xie, F.; Jia, F.; Zhuo, L.; Lu, Z.; Si, L.; Huang, J.; Zhang, M.; Ma, Q. Ultrathin mxene/aramid nanofiber composite paper with excellent mechanical properties for efficient electromagnetic interference shielding. *Nanoscale* **2019**, 11, 48, 23382–23391.
- (19) Zeng, Z.; Chen, M.; Pei, Y.; Seyed Shahabadi, S. I.; Che, B.; Wang, P.; Lu, X. Ultralight and flexible polyurethane/silver nanowire nanocomposites with unidirectional pores for highly effective electromagnetic shielding. *ACS Appl. Mater. Interfaces* **2017**, 9, 37, 32211–32219.
- (20) Chen, W.; Liu, L. X.; Zhang, H. B.; Yu, Z. Z. Flexible, transparent, and conductive $\text{Ti}_3\text{C}_2\text{T}_x$ MXene-silver nanowire films with smart acoustic sensitivity for high-performance electromagnetic interference shielding. *ACS Nano* **2020**, 16643–16653.
- (21) Liu, L. X.; Chen, W.; Zhang, H. B.; Wang, Q. W.; Guan, F.; Yu, Z. Z. Flexible and multifunctional silk textiles with biomimetic leaf-like MXene/silver nanowire nanostructures for electromagnetic interference shielding, humidity monitoring, and self-derived hydrophobicity. *Adv. Funct. Mater.* **2019**, 29, 44.
- (22) Wu, K.; Wang, J.; Liu, D.; Lei, C.; Liu, D.; Lei, W.; Fu, Q. Highly thermoconductive, thermostable, and super-flexible film by engineering 1d rigid rod-like aramid nanofiber/2d boron nitride nanosheets. *Adv. Mater.* **2020**, 32, 8, 1906939.
- (23) Lu, Z.; Si, L.; Dang, W.; Zhao, Y. Transparent and mechanically robust poly (para-phenylene terephthamide) ppta nanopaper toward electrical insulation based on nanoscale fibrillated aramid-fibers. *Compos. Part A-Appl. Sci. Manuf.* **2018**, 115, 321–330.
- (24) Kuang, Q.; Zhang, D.; Yu, J. C.; Chang, Y. W.; Yue, M.; Hou, Y.; Yang, M. Toward record-high stiffness in polyurethane nanocomposites using aramid nanofibers. *J. Phys. Chem. C* **2015**, 119, 49, 27467–27477.
- (25) Lyu, J.; Liu, Z.; Wu, X.; Li, G.; Fang, D.; Zhang, X. Nanofibrous kevlar aerogel films and their phase-change composites for highly efficient infrared stealth. *ACS Nano* **2019**, 13, 2, 2236–2245.